ChemComm

COMMUNICATION

View Article Online
View Journal | View Issue



Cite this: *Chem. Commun.*, 2026, **62**, 510

Received 10th October 2025,
Accepted 24th November 2025

DOI: 10.1039/d5cc05790f

rsc.li/chemcomm



# Chain-length-dependent reactivity of alkenyl phosphates in ruthenium-catalyzed cross-metathesis

Apicha Pontavatchai,[ab] Kevin Schwedtmann,[a] Philipp Royla,[a] Kai Schwedtmann,[a] Tossapol Khamnaen,[c] Uwe Schwarzenbolz,[a] Thomas Henle,[a] Ekasith Somsook *[b] and Jan J. Weigand *[a]

**We report a chain-length-dependent reactivity pattern in the cross-metathesis of alkenyl phosphates catalyzed by the second-generation Grubbs catalyst (GII). While vinyl phosphates undergo unproductive decomposition to generate a ruthenium-carbide complex, extending the alkyl spacer restores productive cross-metathesis. DFT studies rationalize this transformation to occur *via* a proton-coupled phosphate elimination mechanism.**

Olefin cross-metathesis (CM) is a foundational transformation in organic and organometallic chemistry, providing a versatile tool for the construction of complex olefinic motifs.[1–3] The development of ruthenium-based catalysts with high functional group tolerance, notably the second-generation Grubbs catalyst (**GII**), has enabled CM reactions with a broad range of heteroatom-substituted olefins.[4–6] Among these, phosphorus-containing substrates – such as alkenyl phosphonates (**I**) and phosphine oxides (**II**) – have been employed to construct valuable phosphorus-functionalized alkenes (Fig. 1).[7–9] However, alkenyl phosphate esters remain largely unstudied in this context, despite their synthetic accessibility and relevance in flame retardant and lubricant chemistry. In these application areas, the length and substitution pattern of the alkenyl (or alkyl) tether are well known to modulate macroscopic properties such as volatility, polarity, miscibility with polymer matrices and viscosity.[10–12] Thus, being able to control the spacer length in alkenyl phosphates by cross-metathesis is also attractive from an application-oriented perspective. The potential of alkenyl phosphates as CM substrates is intriguing not only for synthetic applications, but also from a mechanistic perspective. The presence of a cleavable phosphate ester group introduces the possibility of catalyst deactivation or alternative reaction pathways, particularly under metathesis conditions involving short-chain vinyl or allyl tethers. Understanding how linker architecture influences reactivity is therefore critical.

Herein, we report a chain-length-dependent reactivity switch in the CM of diethyl alkenyl phosphates catalysed by the second-generation Grubbs catalyst (**GII**). Vinyl phosphate substrates undergo unproductive decomposition to a ruthenium-carbide species, effectively inhibiting metathesis. In contrast, extension of the alkenyl chain (allyl and butenyl derivatives) restores productive CM reactivity. DFT calculations rationalize this switch by invoking a proton-coupled phosphate elimination pathway. These findings highlight how the linker structure modulates the outcome of metathesis reactions involving phosphorus-functionalized olefins, in line with established type-dependent substrate reactivity models.[9,13]

Grubbs and co-workers have categorized olefins into four distinct types based on their reactivity in CM reactions: type I olefins dimerize readily and undergo fast CM; type II olefins are moderately reactive and often benefit from excess type I partners; type III olefins do not homodimerize and typically require

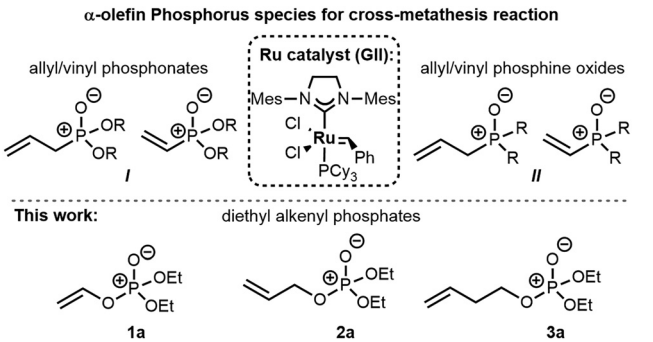


Fig. 1 Representative P-functionalized α-olefins previously studied in cross-metathesis (top) and the diethyl alkenyl phosphates explored in this work (bottom).

[a] *Chair of Inorganic Molecular Chemistry, Technische Universität Dresden, 01069 Dresden, Germany. E-mail: jan.weigand@tu-dresden.de*
[b] *NANOCAST Laboratory, Center for Catalysis for Advanced Sustainable Transformation (CAST), Department of Chemistry and Center of Excellence for Innovation in Chemistry, Faculty of Science, Mahidol University, 272 Rama VI Rd., Ratchathewi, Bangkok 10400, Thailand*
[c] *SCG Chemicals Co.Ltd., 1 Thanon Siam Cement, Bang Sue, Bangkok 10800, Thailand*

more reactive partners; and type IV olefins are essentially unreactive. This classification provides a predictive framework for optimizing cross-selectivity and avoiding undesired side reactions.[1,2,13]

In this study, we examined three alkenyl phosphates of increasing chain length, namely vinyl phosphate (**1a**), allyl phosphate (**2a**), and butenyl phosphate (**3a**) diethyl esters, as substrates for CM with various terminal olefins using the second-generation Grubbs catalyst (**GII**) (Fig. 1). The chosen olefin partners include type I substrates (*e.g.*, styrene, allyl bromide, hexenyl acetate) and borderline type II or II–III olefins (*e.g.*, 1,1-dimethyl allyl alcohol, 5-hexen-2-one, allyl acetate), enabling a nuanced evaluation of cross-metathesis reactivity and selectivity across different electronic and steric profiles.

We started our investigation by reactivity studies of vinyl phosphate **1a** that failed to undergo productive CM under standard reaction conditions (5 mol% **GII**, $CH_2Cl_2$, 45 °C). In all tested combinations with type I olefins, no cross-product formation was observed. Instead, a color change and precipitate formation were noted during the reaction. Subsequent $^{31}P$ NMR analysis revealed two distinct signals: one corresponding to phosphoric acid diethyl ester (**5**) at $\delta$ = 0.9 ppm,[14] and a second resonance at $\delta$ = 34.2 ppm consistent with the formation of a ruthenium-carbide species (**4**).[15]

A stoichiometric reaction of **1a** with **GII** (1 : 1 molar ratio) in the absence of additional olefins gives the same products, confirming that vinyl phosphate **1a** triggers catalyst decomposition (Scheme 1) resembling previous reports of Ru-carbide formation *via* metathesis of vinyl-containing substrates such as vinyl chloride and vinyl acetate, which promote proton transfer and ligand elimination.[16–18] Ru-carbide **4** was isolated from this reaction in 70% yield and its formation was unambiguously verified by X-ray diffraction analysis of suitable single crystals obtained after recrystallization (Fig. S16). To gain mechanistic insight into this decomposition process, we performed DFT calculations on the reaction of **1a** and **GII**.[19] The computed reaction profile (Fig. 2) shows that the Ru-vinyl phosphate intermediate (**R1a**) is initially formed by a regular ligand exchange process under the elimination of styrene (**6**) in an exergonic transformation ($\Delta G$ = −6.9 kcal mol$^{-1}$).

This intermediate then readily eliminates the phosphate group by a concerted intramolecular proton transfer mechanism (transition state **TS1a**) from the carbene carbon to the phosphate oxygen, which is accompanied by cleavage of the elongated C–O bond (2.14 Å). The product of this transformation is encounter complex **P1a** of the terminal Ru-carbide complex **4** and diethyl phosphoric acid (**5**). The barrier for this transformation ($\Delta G^{\ddagger}$ = 17.1 kcal mol$^{-1}$) is readily surmountable under the reaction conditions and the resulting dissociated products are significantly stabilized ($\Delta G$ = −13.0 kcal mol$^{-1}$) compared to the starting materials, supporting the experimental observation that metathesis reactions with **1a** are completely suppressed.[20] This represents the first high-yielding preparation of a Ru–carbide complex from a vinyl phosphate offering an efficient alternative to existing synthetic strategies for accessing well-defined carbide species.[20–22]

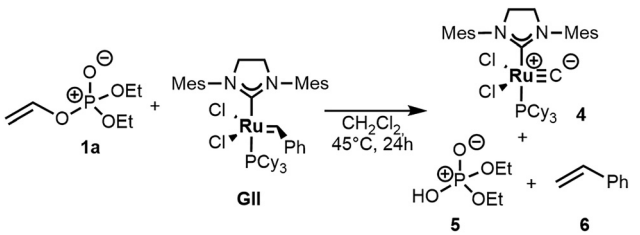


Scheme 1 Reaction of vinyl phosphate **1a** with **GII** catalyst, leading to Ru-carbide complex **4**, diethyl phosphate (**5**), and styrene (**6**) *via* proton-coupled elimination.

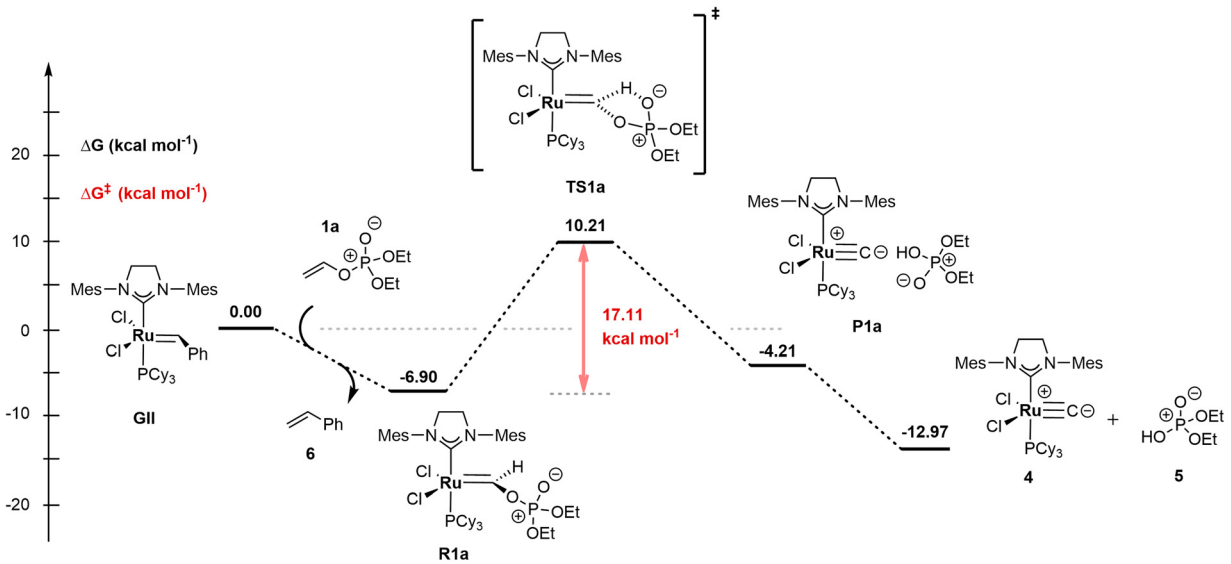


Fig. 2 Computed free energy profile for the reaction of vinyl phosphate **1a** with the second-generation Grubbs catalyst (**GII**), showing a proton-coupled elimination leading to Ru-carbide formation. The key transition state **TS1a** ($\Delta G^{\ddagger}$ = 17.1 kcal mol$^{-1}$) involves intramolecular proton transfer, and the final Ru-carbide product (**4**) is thermodynamically favoured ($\Delta G$ = −13.0 kcal mol$^{-1}$), consistent with experimental catalyst deactivation.

Table 1 Cross-metathesis of chain-length-varied diethyl allyl phosphate (**2a**) and diethyl butenyl phosphate (**3a**) with representative terminal olefins (**a–h**) using **GII** catalyst

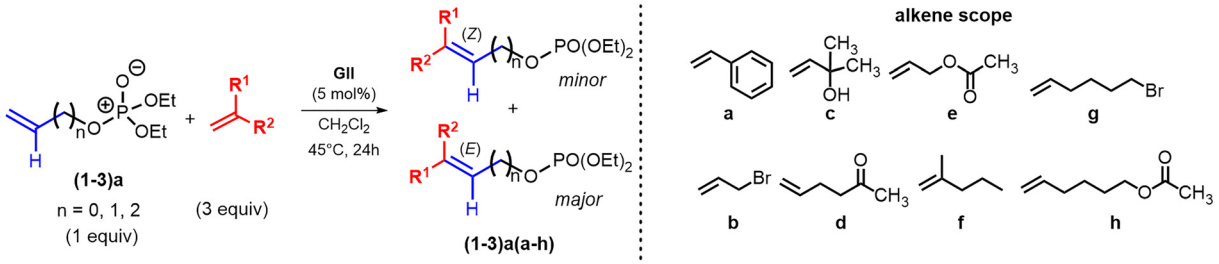


| Entry | Olefin substrate | Type | $R^1$ | $R^2$ | Product from **2a** | Yield (%) | *E*/*Z* | Product from **3a** | Yield (%) | *E*/*Z* |
|---|---|---|---|---|---|---|---|---|---|---|
| 1 | **a** (styrene) | I | H | Ph | **2aa** | 35 | 100 : 0 | **3aa** | 50 | 100 : 0 |
| 2 | **b** (allyl bromide) | I | H | $CH_2Br$ | **2ab** | 42 | 93 : 7 | **3ab** | 73 | 91 : 9 |
| 3 | **c** (Me-allyl alcohol) | II–III | H | $C(CH_3)_2OH$ | **2ac** | 56 | 100 : 0 | **3ac** | 84 | 100 : 0 |
| 4 | **d** (5-hexen-2-one) | II–III | H | $C_2H_4COCH_3$ | **2ad** | 23 | 91 : 9 | **3ad** | 65 | 85 : 15 |
| 5 | **e** (allyl acetate) | II–III | H | $CH_2OAc$ | **2ae** | 40 | 91 : 9 | **3ae** | 49 | 87 : 13 |
| 6 | **f** (2-methylpent-1-ene) | Borderline type IV | $CH_3$ | $C_3H_7$ | **2af** | 7 | 63 : 37 | **3af** | 50 | 68 : 32 |
| 7 | **g** (6-bromo hexene) | I | H | $C_4H_8Br$ | **2ag** | 62 | 86 : 14 | **3ag** | 73 | 87 : 13 |
| 8 | **h** (hexenyl acetate) | I | H | $C_4H_8OAc$ | **2ah** | 66 | 93 : 7 | **3ah** | 70 | 85 : 15 |

Yields refer to isolated products after chromatography. Olefin type classification based on Grubbs *et al.*[1,2]

A contrasting reactivity is observed using diethyl allyl phosphate (**2a**) and diethyl butenyl phosphate (**3a**) as CM substrates with a representative set of terminal alkenes, indicating that spatial separation between the reactive olefin and phosphate group is crucial to prevent unproductive elimination. Both **2a** and **3a** successfully underwent cross-metathesis under standard conditions (5 mol% **GII**, $CH_2Cl_2$, 45 °C, 24 h), giving the desired cross-products in moderate to good yields across a range of terminal alkenes with differing electronic and steric profiles (Table 1).

Diethyl allyl phosphate (**2a**) exhibited productive cross-metathesis with all tested partners. Generally, the conversions proceeded in favor of the *E*-isomers, although with some alterations in sterically encumbered cases. Nonetheless, the conversions were accompanied by significant side reactions reflecting the moderate reactivity of **2a** and its susceptibility to competitive side processes. In particular, the formation of diethyl phosphoric acid was consistently observed by $^{31}P$ NMR ($\delta$ = 0.9 ppm),[14] indicating partial phosphate elimination. Additionally, the formation of homodimers derived from **2a** was observed in several cases, particularly in reactions involving less reactive or sterically hindered olefins (*e.g.*, methyl acrylate, 2-methylpent-1-ene). Notably, to support identification of the side products, the homodimers of **2a** and **3a** were independently prepared and isolated applying the same catalytic conditions under the absence of any other olefin (see SI, S2.24 and S2.25).

Butenyl phosphate (**3a**) exhibited superior CM performance. Isolated yields were generally higher, and side products, including homodimers and phosphate-derived elimination products, were markedly suppressed. These findings suggest that the increased chain length between the olefin and the phosphate ester decouples their reactivity, reducing the likelihood of intramolecular proton-coupled elimination. This effect is further supported by the excellent cross-selectivity and high *E*/*Z* ratios observed across all tested olefins. The terminal alkenes employed in this study span a range of reactivity types according to the Grubbs classification (type I–IV olefins). With type I olefins (*e.g.*, styrene, ally bromide, hexenyl acetate), both **2a** and **3a** undergo efficient cross-metathesis, though **3a** delivers consistently higher yields and cleaner product profiles. Type II–III olefins (*e.g.*, 1,1-dimethyl allyl alcohol, 5-hexen-2-one, allyl acetate) show reduced reactivity and are prone to inducing homodimer formation with **2a**. Reactions involving borderline type IV partners (*e.g.*, 2-methylpent-1-ene) generally result in low conversion and diminished selectivity.

Interestingly, the phosphate substrates themselves (**1–3**)**a** can also be considered in light of this classification. Vinyl phosphate **1a** shows no homodimerization and undergoes irreversible catalyst decomposition – features characteristic of a type IV olefin. Allyl phosphate **2a** displays moderate reactivity, competes with dimer formation, and is thus best described as type II–III. Butenyl phosphate **3a**, in contrast, consistently undergoes productive CM and shows partial homodimerization, fitting a type I–II hybrid classification.

This extension of the Grubbs classification to heteroatom-substituted olefins enables a more predictive framework for understanding and optimizing phosphorus-containing metathesis systems. Together, these findings underscore that both the alkene partner and the phosphate substrate influence the CM reaction outcome. The combination of steric accessibility, chain length, and electronic activation governs whether productive CM or unproductive decomposition dominates. These observations also align well with the mechanistic picture provided by DFT analysis (Fig. 2). With **1a**, close orbital alignment facilitates phosphate elimination and Ru-carbide formation. In **2a**, this interaction remains partially accessible, while in **3a**, the phosphate motif is sterically and electronically decoupled from the carbene center, thus promoting productive CM turnover. The computed frontier orbitals of the respective Ru-carbene intermediates support this trend (Fig. 3 and Fig. S74 in the SI).

 

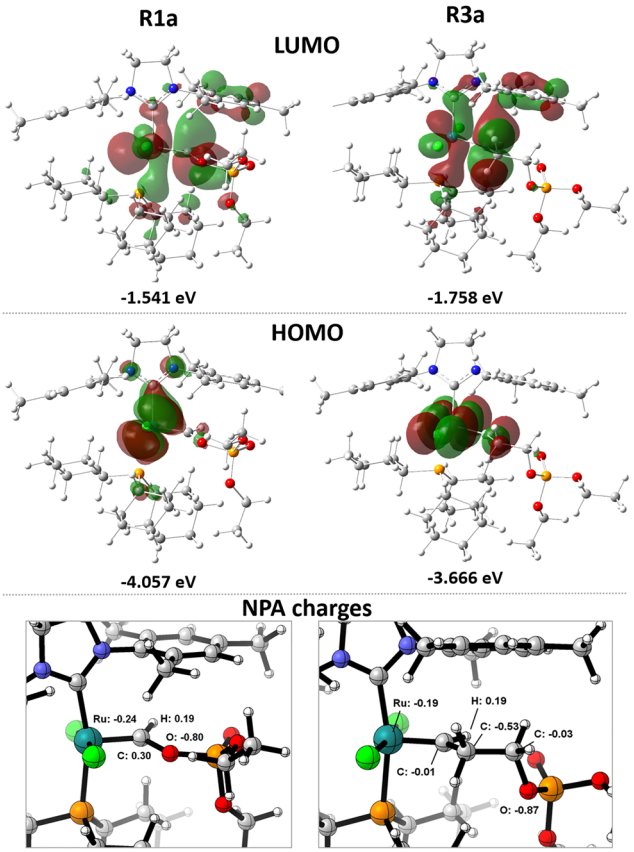


Fig. 3 DFT Optimized structures (M06L/def2-SVP) and frontier molecular orbitals (LUMO and HOMO) of Ru–carbene intermediates derived from vinyl (**1a**), and butenyl (**3a**) phosphate substrates and NPA charges of the atoms near the reactive center.

In the case of **R1a**, the LUMO exhibits significant orbital density on the phosphate group and is destabilized compared to the LUMO in **R2a** and **R3a**. Natural population analysis charges (Fig. 3 and Fig. S75) reveal a positive charge on the carbene carbon in **R1a** (+0.30) that facilitates deprotonation of the α-hydrogen atom leading to phosphate elimination and Ru-carbide formation, consistent with experimental observation.

In contrast, a clear spatial separation between the phosphate group and the reactive carbene center in both HOMO and LUMO is observed for **2a** and **3a** along with a near neutral charge at the carbene carbon atom, which correlates with the improved catalytic performance and suppression of decomposition.

In summary, we have identified a clear chain-length dependence in the reactivity of alkenyl phosphate substrates in Ru-catalyzed cross-metathesis. The vinyl derivative **1a** undergoes a distinct decomposition pathway, forming a Ru-carbide species *via* phosphate-assisted proton transfer. This reactivity is suppressed in longer-chain analogues **2a** and **3a**, where productive CM is restored. These findings highlight the importance of spatial separation between reactive groups and extend the Grubbs-type reactivity classification to phosphate-functionalized olefins. From an application perspective, the ability to access allyl- *versus* butenyl-phosphate products by CM allows to tune physical properties in phosphate-based flame retardants and lubricant additives, such as volatility, miscibility and viscosity that are spacer-length dependent. We anticipate that these insights will support future design principles for phosphorus-modified olefin metathesis reactions.

A. P., E. S., and J. J. W. conceptualized the study; A. P. conducted the syntheses, characterization, DFT calculations, data analysis, visualization and writing of the original draft; K. S. performed experimental support, single-crystal X-ray structure determination, and data validation; U. S. contributed analytical investigations and data validation; P. R. supervised experimental work and contributed mechanistic discussion, data interpretation and writing of the original draft; K. S. and J. J. W. conceived, oversaw, and directed the project; T. K. contributed conceptual support, resources, and industrial perspective; T. H. supervised analytical work and provided resources; E. S. supervised research in Thailand and contributed resources and scientific discussion; T. K. and J. J. W. secured funding. All authors contributed to data analysis, manuscript review and editing, and scientific discussion.

We thank the German Research Foundation (DFG) for financial support through the Reinhart Koselleck Grant (WE 4621/10-1). A. P. acknowledges financial support through the ERASMUS+ mobility program. We are also grateful to Siam Cement Group Chemicals Public Company Limited (SCG Chemicals) for generous funding.

## Conflicts of interest

There are no conflicts to declare.

## Data availability

The data supporting this article have been included as part of the supplementary information (SI). Supplementary information: syntheses and analyses, NMR spectra, crystallographic details including ORTEP representations, details for the DFT calculations including XYZ-files.

CCDC 2493579 contains the supplementary crystallographic data for this paper.[23]

## Notes and references

1 H. E. Blackwell, D. J. O'Leary, A. K. Chatterjee, R. A. Washenfelder, D. A. Bussmann and R. H. Grubbs, *J. Am. Chem. Soc.*, 2000, **122**, 58–71.
2 S. J. Connon and S. Blechert, *Angew. Chem., Int. Ed.*, 2003, **42**, 1900–1923.
3 R. H. Grubbs, *Tetrahedron*, 2004, **60**, 7117–7140.
4 M. Scholl, S. Ding, C. W. Lee and R. H. Grubbs, *Org. Lett.*, 1999, **1**, 953–956.
5 T. M. Trnka and R. H. Grubbs, *Acc. Chem. Res.*, 2001, **34**, 18–29.
6 B. F. Straub, *Angew. Chem., Int. Ed.*, 2005, **44**, 5974–5978.
7 A. K. Chatterjee, T.-L. Choi and R. H. Grubbs, *Synlett*, 2001, 1034–1037.
8 F. Bisaro and V. Gouverneur, *Tetrahedron Lett.*, 2003, **44**, 7133–7135.
9 O. M. Demchuk, K. M. Pietrusiewicz, A. Michrowska and K. Grela, *Org. Lett.*, 2003, **5**, 3217–3220.
10 S. V. Levchik and E. D. Weil, *Polym. Adv. Technol.*, 2005, **16**, 707–716.
11 I. van der Veen and J. de Boer, *Chemosphere*, 2012, **88**, 1119–1153.
12 D. W. Johnson and J. E. Hils, *Lubricants*, 2013, **1**, 132–148.
13 A. K. Chatterjee, T.-L. Choi, D. P. Sanders and R. H. Grubbs, *J. Am. Chem. Soc.*, 2003, **125**, 11360–11370.
14 I. Lukes, M. Borbaruah and L. D. Quin, *J. Am. Chem. Soc.*, 1994, **116**, 1737–1741.

15 R. G. Carlson, M. A. Gile, J. A. Heppert, M. H. Mason, D. R. Powell, D. V. Velde and J. M. Vilain, *J. Am. Chem. Soc.*, 2002, **124**, 1580–1581.
16 S. R. Caskey, M. H. Stewart, J. E. Kivela, J. R. Sootsman, M. J. Johnson and J. W. Kampf, *J. Am. Chem. Soc.*, 2005, **127**, 16750–16751.
17 M. L. Macnaughtan, M. J. Johnson and J. W. Kampf, *J. Am. Chem. Soc.*, 2007, **129**, 7708–7709.
18 C. Buda, S. R. Caskey, M. J. Johnson and B. D. Dunietz, *Organometallics*, 2006, **25**, 4756–4762.
19 For details see SI.
20 A. Hejl, T. M. Trnka, M. W. Day and R. H. Grubbs, *Chem. Commun.*, 2002, 2524–2525.
21 A. Reinholdt, J. E. Vibenholt, T. J. Morsing, M. Schau-Magnussen, N. E. A. Reeler and J. Bendix, *Chem. Sci.*, 2015, **6**, 5815–5823.
22 T. J. Morsing, A. Reinholdt, S. P. Sauer and J. Bendix, *Organometallics*, 2016, **35**, 100–105.
23 CCDC 2493579: Experimental Crystal Structure Determination, 2025, DOI: **10.5517/ccdc.csd.cc2pps17**.